Selective Hydrogenation of 1,3-Butadiene to 1-Butene by Pd(0) Nanoparticles Embedded in Imidazolium Ionic Liquids

Alexandre P. Umpierre,[a] Giovanna Machado,[a] Gerhard H. Fecher,[b] Jonder Morais,[c] Jairton Dupont[a,*]

[a] Laboratory of Molecular Catalysis, Institute of Chemistry, UFRGS, Av. Bento Gonçalves 9500, Porto Alegre, 91501-970, RS, Brazil
Fax: (+55)-51-3316-7304, e-mail: dupont@iq.ufrgs.br
[b] Institut für Anorganische und Analytische Chemie, Johannes-Gutenberg Universität, 55099 Mainz, Germany
[c] Institute of Physics, UFRGS, Av. Bento Gonçalves 9500, Porto Alegre, 91501-970, RS, Brazil

Received: October 11, 2004; Revised: April 18, 2005; Accepted: April 29, 2005

Abstract: The reduction of $Pd(acac)_2$ (acac = acetylacetonate), dissolved in 1-*n*-butyl-3-methylimidazolium hexafluorophosphate ($BMI \cdot PF_6$) or tetrafluoroborate ($BMI \cdot BF_4$) ionic liquids, by molecular hydrogen (4 atm) at 75 °C affords stable, nanoscale Pd(0) particles with sizes of 4.9 ± 0.8 nm. Inasmuch as 1,3-butadiene is at least four times more soluble in the $BMI \cdot BF_4$ than butenes, the selective partial hydrogenation could be performed by Pd(0) nanoparticles embedded in the ionic liquid. Thus, the isolated nanoparticles promote the hydrogenation of 1,3-butadiene to butenes under solventless or multiphase conditions. Selectivities up to 97% in butenes were observed in the hydrogenation of 1,3-butadiene by Pd(0) nanoparticles embedded in $BMI \cdot BF_4$ under mild reaction conditions (40 °C and 4 atm of hydrogen at constant pressure). Selectivities up to 72% in 1-butene were achieved at 99% 1,3-butadiene conversion, 40 °C and 4 atm of constant pressure of hydrogen. The amounts of butane (fully hydrogenated 1,3-butadiene) and *cis*-2-butene products are marginal and the butenes do not undergo isomerisation process, indicating that the soluble Pd(0) nanoparticles possess a pronounced surface-like rather than homogeneous-like catalytic properties.

Keywords: dienes; hydrogenation; ionic liquids; nanoparticles; palladium

Introduction

The production of polymer-grade 1-butene through the selective hydrogenation of 1,3-butadiene is an important industrial process since even traces of 1,3-butadiene can poison the olefin polymerization catalysis and consequently reduce the total polymer production. The hydrogenation process for the generation of rich streams in 1-butene can be accomplished by a plethora of palladium catalysts. Supported palladium catalysts such as Pd/SiO_2 and Pd/alumina, usually in the presence of promoters or modifiers,[1] are among the most used and investigated catalysts for the partial hydrogenation of 1,3-butadiene. In this respect, the catalytic activity and selectivity can be strongly influenced by the metal dispersion, the nature of the support and the preparation method. In particular, in these catalytic processes the selectivity in 1-butene is reduced due to the parallel isomerisation of 1-butene to internal butenes and total diene hydrogenation, which limit the overall yield in 1-butene. The most accepted mechanism involves adsorption of the butadiene through di-π-coordination. The 1,2- or 1,4-H addition on the diene produces 1-butene or 2-butenes, respectively. The *trans/cis* 2-butenes ratios are the direct result of the interconversion between the diene conformer-adsorbed species on the Pd surface. The *trans*-2-butene is formed preferentially since the *S-trans* conformer is much more stable than the *S-cis* conformer. Moreover, the isomerisation of the monoenes formed is suppressed in the presence of an excess of the diene .[2] An alternative mechanism, involving the formation of carbenes, has been proposed in cases where the observed ratios of *trans/cis*-2-butenes are comparable and *n*-butane is formed as direct product of the diene hydrogenation.[3]

Transition metal complexes based on palladium or cobalt, either in homogenous or multiphase conditions, are also known to catalyse the partial hydrogenation of 1,3-butadiene with high selectivity in butenes, but only moderate yields in 1-butene were achieved.[4] For these monometallic catalysts the proposed mechanism involves also the formation of a stable π-allyl intermediate (regardless of the H_2 cleavage mechanism) through the M–H addition to a conjugated diene. The isomerisation of the 1-butene formed in the internal butenes is characteristic of the involvement of "homogeneous" M–H spe-

  DOI: 10.1002/adsc.200404313

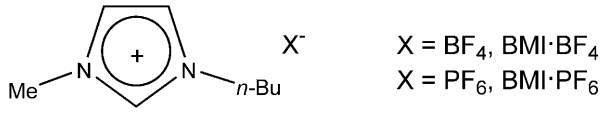

Figure 1. BMI·BF_4 and BMI·PF_6 imidazolium ionic liquids.

cies.[5] Therefore, at least in the case of Pd catalysts, the product selectivity in the partial hydrogenation of butadiene can be used as a chemical probe to get some insights into the nature of their catalytically active sites, i.e., if they are characteristic "homogeneous" (single site) or "heterogeneous" (multi-site) sites.

Among the multiphase catalytic systems, those based on Pd(II) compounds dissolved in 1-*n*-butyl-3-methylimidazolium hexafluorophosphate (BMI·PF_6) or tetrafluoroborate (BMI·BF_4) ionic liquids[6] (Figure 1) yield butenes in 95% selectivity at 98% butadiene conversion. The higher selectivity in butenes obtained under multiphase catalysis compared with those performed in homogeneous conditions was attributed to the higher solubility of butadiene in the ionic phase than that of butenes.[7] Moreover, the isomerisation of the 1-butene formed in 2-butenes occurred even at very low 1,3-butadiene conversions.

It is clear that both heterogeneous and homogeneous palladium catalysts can promote the partial hydrogenation of 1,3-butadiene to butenes. Moreover, with some modifications, such as the addition of additives in the case of supported Pd catalysts, or the use of multiphase catalysis in the case of Pd complexes, one can improve the yield in 1-butene. It is expected that soluble transition-metal nanoparticles of 1–10 nm in size will exhibit physical-chemical properties intermediate between those of the smallest element from which they can be composed and those of the bulk material.[8] However, the use of soluble Pd(0) nanoparticles[9,10] as catalysts for the hydrogenation of dienes has been only marginally explored for cyclohexadiene.[11] It was therefore of interest to check if soluble Pd(0) nanoparticles could perform the selective partial hydrogenation of 1,3-butadiene. We wish to disclose herein that indeed Pd(0) nanoparticles of 4.9 ± 0.8 nm embedded in BMI·BF_4 ionic liquid are highly efficient multiphase catalysis for the generation of 1-butene in up to 72% yield from the partial hydrogenation of 1,3-butadiene.

Results and Discussion

Preparation and Characterisation of the Pd(0) Nanoparticles

The Pd(0) nanoparticles have been prepared by the simple reduction of Pd(II) compound dissolved in ionic liquids, a method that was recently developed for the generation of stable Ir, Rh and Ru nanoparticles of 2–4 nm in size.[12] Thus, the treatment of a solution of $Pd(acac)_2$ dissolved in 1 mL of BMI·PF_6 with molecular hydrogen (4 atm, constant pressure) at 75 °C for 5 minutes affords a black solution from which a black powder is isolated by centrifugation (3000 rpm, 15 min, 3 times). The isolated black powder was washed with methanol, dried under reduced pressure and analysed by X-ray diffraction (XRD), X-ray photoelectron spectroscopy (XPS), transmission electron microscopy (TEM), and energy dispersive spectroscopy (EDS).

The X-ray diffraction patterns could be adjusted to the predicted lines of the Pd fcc structure (Figure 2). The indexation of Bragg reflections was obtained by a pseudo-Voigt profile fitting using the FULLPROF code. The most representative reflections to Pd(0) were indexed as closed face-centred packing and the cell unit parameter obtained was $a = 0.38979$ nm. The Bragg reflections at 40.141^0, 46.623^0, 68.176^0, 82.082^0, and 86.579^0 correspond to the indexed planes of the crystals of Pd(0) (111), (200), (011), (220), (311) and (222).

The diffraction ring patterns (Figure 3a) from selected area diffraction (SAD) confirmed the crystalline nature of the particles. Moreover, the presence of Pd in the sample was also confirmed by the energy dispersion spectrum (EDS, Figure 3b).

The XPS analysis showed the presence of palladium, fluorine, carbon and a small contribution of phosphorus. It is clear that the F and P signals indicate that the nanoparticles (black powder) contain residues from the ionic liquid. It is worth pointing out that the valence band (4d, 5 s) emission occurs at a binding energy of *ca.* 0–8 eV, measured with respect to the Fermi level, which is quite similar to that of pure Pd. No other impurities were de-

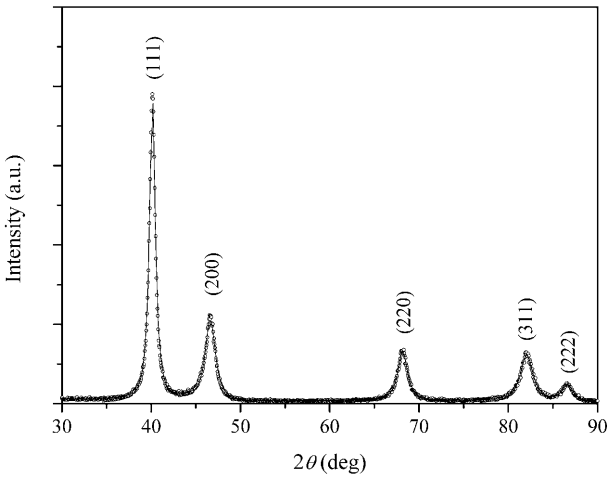

Figure 2. X-ray diffraction pattern of Pd(0) nanoparticles synthesised from dissolved $Pd(acac)_2$ in BMI·PF_6 treated with molecular hydrogen (4 atm) at 75 °C for 5 minutes. The peaks are labelled with the hkl of the planes for the corresponding Bragg angles.

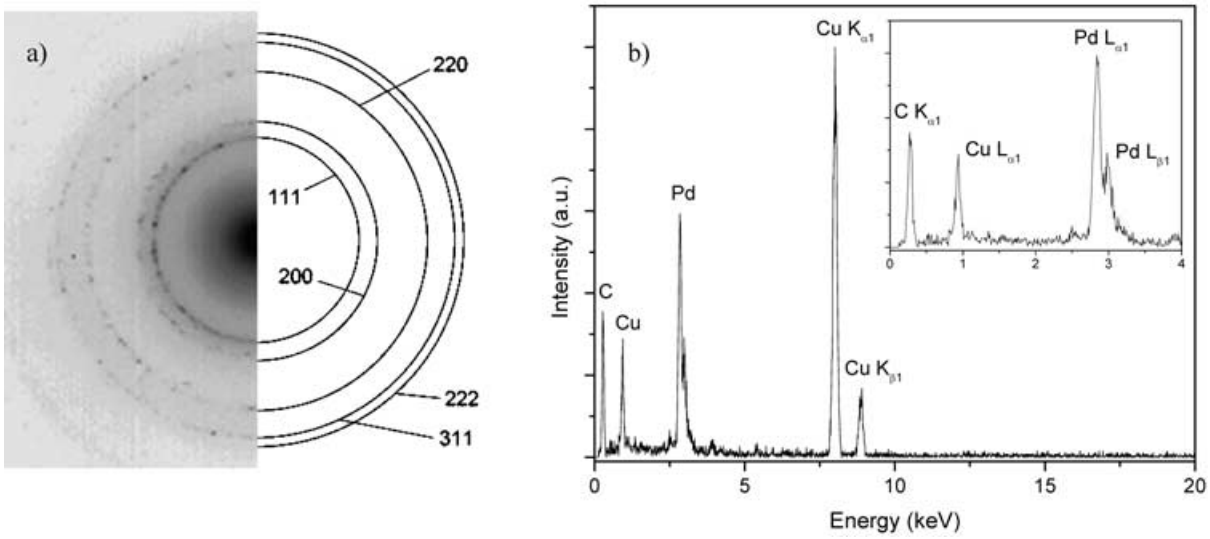

Figure 3. a) Selected area diffraction (SAD, *left*) of Pd(0) nanoparticles synthesised from dissolved $Pd(acac)_2$ in $BMI \cdot PF_6$ treated with molecular hydrogen (4 atm) at 75 °C for 5 minutes (left) and the simulated rig pattern for Pd(0) (*right*). **b)** Energy dispersion spectrum (EDS) of the sample of Figure 5 confirming the presence of palladium in the sample.

tected within the sensitivity of the technique. Figure 4 shows the XPS signal of the Pd 3d and F 1 s regions (inset). The Pd 3d spectrum indicates the presence of two chemical states of Pd at the nanoparticle surface with distinct binding energies; the main contribution is related to Pd(0) (Pd–Pd bonds, $Pd^{5/2}$ at 335 eV) and the other corresponding to Pd–F bonds ($Pd^{5/2}$ at 336.7 eV). It was found that the relation between the Pd–Pd and the Pd–F areas in the spectrum is about 2.8, which corresponds to a 74% contribution of Pd–Pd bonds and 26% of Pd–F bonds on the nanoparticle surface. This result is a strong indication of the effective interaction of ionic liquid with the metal surface that may be responsible for the stabilisation of the nanoparticles.

Inasmuch as imidazolium ionic liquids possess no measurable vapour pressure and a relatively high viscosity (2–3 Poises) the nanoparticle's size and morphology could be investigated *in situ* by transmission electron microscopy (TEM). Thus, the isolated Pd(0) material was re-dispersed in the $BMI \cdot PF_6$ ionic liquid and placed as a thin film in a carbon coated copper grid and analysed by TEM (Figure 5a). The metal particle size distribution was estimated from the measurement of around 300 particle diameters, assuming a spherical shape, found in an arbitrarily chosen area in enlarged microphotographs. These particles display a mono-modal size distribution with an average diameter of (4.9 ± 0.8) nm (Figure 5b), which is in good agreement with the mean diameter estimated from the XRD data.

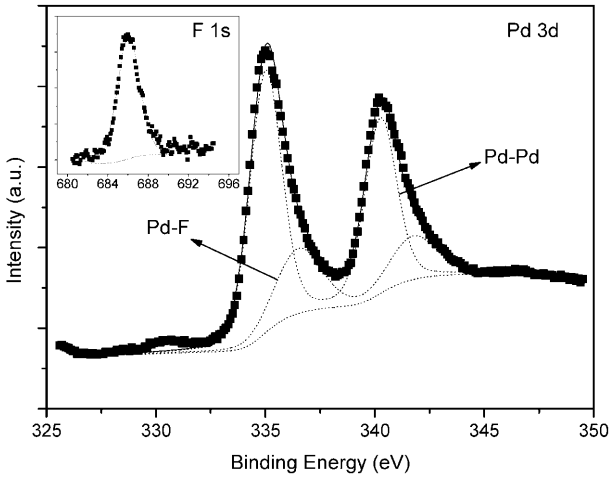

Figure 4. X-ray photoelectron spectra of the of Pd(0) nanoparticles synthesised from $Pd(acac)_2$ dissolved in $BMI \cdot PF_6$ showing the Pd 3d and F 1 s regions (inset) with the fitting results. The Pd 3d doublet presents two components corresponding to Pd–Pd and Pd–F bonds, the first being the most abundant one.

Hydrogenation of 1,3-Butadiene

The hydrogenation of 1,3-butadiene was performed with the isolated Pd(0) either embedded in different amounts of $BMI \cdot BF_4$ and $BMI \cdot PF_6$ or under solvent-free conditions. The use of *in situ* nanoparticles in the ionic liquid is not recommended since it may contain soluble $Pd(acac)_2$ that was not completely reduced and the ionic phase is slightly acid. The initial temperature was set at 40 °C and the hydrogen pressure at 4 atm (constant pressure). The reaction products (Scheme 1) were monitored by GC and the 1,3-butadiene conversion and products selectivity, using Pd(0) nanoparticles embedded in $BMI \cdot BF_4$ and under solvent-free conditions are presented in Figures 6–8.

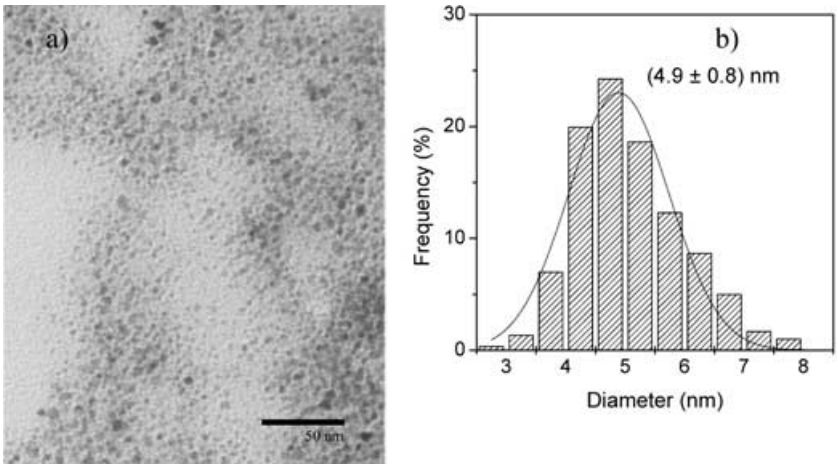

Figure 5. a) TEM micrograph of Pd(0) nanoparticles synthesised from $Pd(acac)_2$ dissolved in $BMI \cdot PF_6$ treated with molecular hydrogen (4 atm) at 75 °C for 5 minutes, supported on a carbon coated grid, and **b)** the corresponding size distribution histogram.

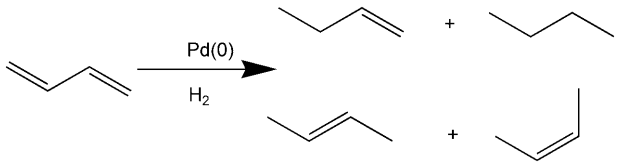

Scheme 1. Products resulting from the hydrogenation of 1,3-butadiene by Pd(0) nanoparticles.

It is clear that the reaction performed under solvent-free conditions is much faster than that performed under biphasic conditions, i.e., the total consumption of butadiene takes less than 2 hours using the isolated Pd(0) nanoparticles whereas almost 6 hours are necessary in the case of the nanoparticles dispersed in the ionic liquid (Figure 6).

This difference is probably related with the typical biphasic nature of the reactions performed in the presence of the ionic liquid that are mass transfer controlled processes as observed in various other related studies.[4] Indeed, the amount of ionic liquid has a strong influence on the catalytic activity in the hydrogenation of 1,3-butadiene by the Pd(0) nanoparticles (Figure 7). In fact the amount of ionic liquid can be reduced to 5×10^{-7} mL without a change in butene selectivity.

The products selectivity is also strongly influenced by the nature reaction media. The formation of butane is almost negligible (less than 2%) in the reactions performed with the Pd(0) nanoparticles embedded in the ionic liquid at any 1,3-butadiene conversion whereas those performed under solvent-free conditions generate significant amounts of the alkane even at low 1,3-butadiene conversions (Figure 8). Noteworthy, 98% selectivity in butenes (72% in 1-butene) is attained at complete 1,3-butadiene conversion. Moreover, the amount of *cis*-2-butene is also negligible in the case of hydrogenation using the nanoparticles embedded in the ionic liquid

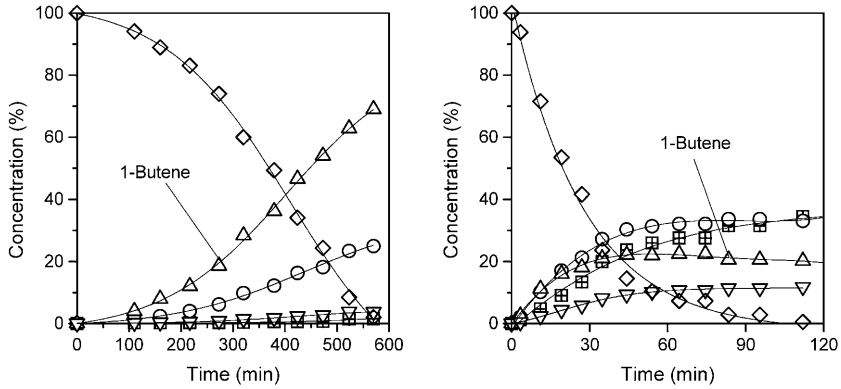

Figure 6. Activity data from the hydrogenation of 1,3-butadiene (2.7 g of 1,3-butadiene) at 40 °C and 4 atm catalysed by Pd(0) nanoparticles (5 mg) embedded in 1×10^{-5} mL of $BMI \cdot BF_4$ (left) and under heterogeneous conditions (right). Legend: ($\diamond$) = 1,3-butadiene, (Δ) = 1-butene, ($\bigcirc$) = *trans*-2-butene, (∇) = *cis*-2-butene, ($\boxplus$) = *n*-butane.

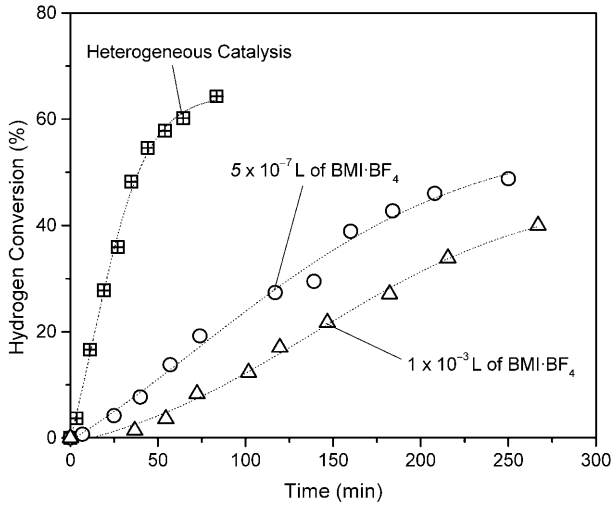

Figure 7. Hydrogenation of 1,3-butadiene (2.7 g of 1,3-butadiene) at 40 °C and 4 atm catalysed by Pd(0) nanoparticles (5 mg) in heterogeneous system and with the nanoparticles embedded in $BMI \cdot BF_4$.

and less than one quarter of the butenes formed under "solvent-free conditions".

Moreover, in the reaction performed with the nanoparticles embedded in $BMI \cdot BF_4$ the formed butenes do not undergo isomerisation, i.e., the selectivity does not change with the diene consumption (Figure 9). This result is in sharp contrast to the catalytic performance observed in the same reaction promoted by Pd(II)[I] compounds dissolved in imidazolium ionic liquids in which the formed 1-butene is isomerised in 2-butenes even in the early stages of the process.[7]

Under "solvent-free" conditions the isomerisation of the formed butenes only occurs in the absence of the diene, i.e., after complete 1,3-butadiene conversion. This was further corroborated by performing the hydrogenation of 1-butene and *trans*-2-butene in a separate set of experiments (Figure 10) using the same reaction conditions employed in the hydrogenation of butadiene.

These patterns of selectivity, i.e., negligible formation of *cis*-2-butenes and the absence of butenes isomerisation in the presence of the diene, indicate that ionic liquid-soluble palladium nanoparticles behave as "heterogeneous-like" (multisite, Scheme 2) rather than "homogeneous-like" (single site) catalysts. The higher selectivity in butenes attained in the reactions performed with the Pd(0) nanoparticles embedded in $BMI \cdot BF_4$, compared with those performed under solvent-free conditions can be related to the greater miscibility of the 1,3-butadiene with the ionic liquid than butenes. Indeed, 1,3-butadiene is at least three times more soluble in $BMI \cdot BF_4$ than butenes at 40 °C.

The partial hydrogenation of 1,3-butadiene could also be performed with the Pd(0) nanoparticles embedded in $BMI \cdot PF_6$ (Figure 11). However, in this case the formation of butane is higher (more than 3 times than those performed by Pd(0) embedded in $BMI \cdot BF_4$) and probably is a result of the less pronounced difference in the miscibility of 1,3-butadiene over butenes.[6a] Noteworthy, the addition of water to the catalytic system does not cause any significant changes in the reaction selectivity.

It is worth noting that the recovered Pd(0) ionic liquid phase can be reused without any significant changes in 1-butene selectivity (Figure 12).

Even though the selectivity of this system suffered no appreciable modification after four charges of 1,3-butadiene, the catalytic activity was somewhat irreproducible, possibly due to expulsion of the catalyst from the reactive phase by stirring and adherence of the nanoparticles to the inner walls of the reactor bottle. At 90% 1,3-butadiene conversion, the turnover frequency (TOF) of the 1,3-butadiene hydrogenation reactions oscillates be-

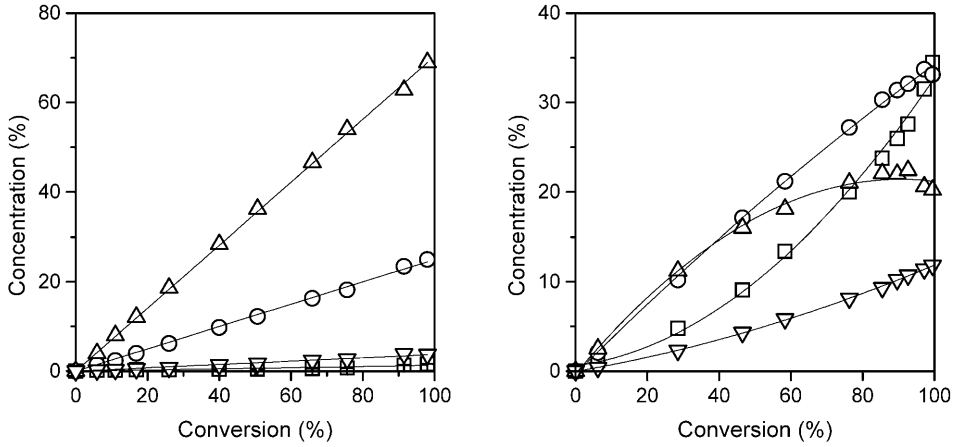

Figure 8. Selectivity data from the hydrogenation of 1,3-butadiene (2.7 g of 1,3-butadiene) at 40 °C and 4 atm catalyzed by Pd(0) nanoparticles (5 mg) embedded in 1×10^{-5} mL of $BMI \cdot BF_4$ (*left*) and under heterogeneous conditions (*right*). Legend: (Δ) = 1-butene, (○) = *trans*-2-butene, (▽) = *cis*-2-butene, (□) = *n*-butane.

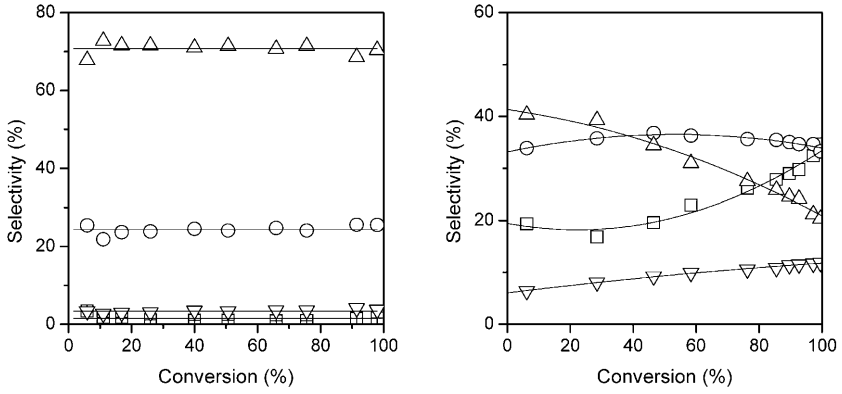

Figure 9. Reaction products selectivity obtained from the hydrogenation of 1,3-butadiene (2.7 g of 1,3-butadiene) at 40 °C and 4 atm catalysed by Pd(0) nanoparticles (5 mg) embedded in 1×10^{-5} mL of BMI·BF_4 (left) and under heterogeneous conditions (right). Legend: (Δ) = 1-butene, (○) = *trans*-2-butene, (▽) = *cis*-2-butene, (□) = *n*-butane.

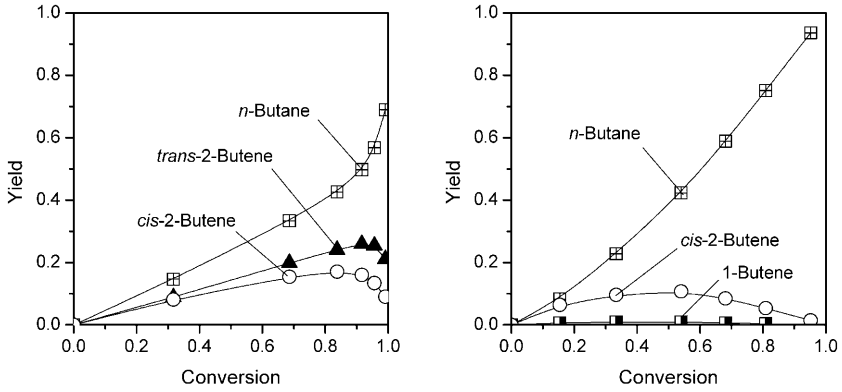

Figure 10. Hydrogenation of 1-butene (*left*) and 2-*trans*-butene (*right*) at 40 °C and 4 atm catalysed by Pd(0) nanoparticles.

tween 30 h^{-1} and 55 h^{-1}. TEM analysis of nanoparticles after the hydrogenation shows significant agglomeration into larger nanoparticles of about 20 nm in diameter (Figure 13). This result indicates that the ionic liquid does not provide an effective protection against agglomeration for the Pd(0) nanoparticles under the catalytic reaction conditions.

It is interesting to point out that under the same reaction conditions (1×10^{-3} mL of BMI·BF_4, 40 °C, 4 atm H_2) the selectivity for butenes, during the hydrogenation of 1,3-butadiene by the classical heterogeneous catalyst Pd/C (5% Degussa), is very low even at relatively low substrate conversions (62% and 61% 1,3-butadiene conversion). This result is an indication that the selectivity for butenes is also related to the nature of the catalysts precursor and that "ionic-liquid-soluble" Pd nanoparticles are superior to the classical heterogeneous Pd/C catalyst.

Conclusion

In summary, we have demonstrated that Pd(0) nanoparticles with relatively small diameters and narrow size distributions can be prepared by simple hydrogen reduction of $Pd(acac)_2$ dispersed in BMI·PF_6 ionic liquid. The XPS analysis showed the effective interaction of ionic liquid with the metal surface that may be responsible for the stability of the nanoparticles. The ionic liquid creates an external layer around the metal nanoparticles that controls the access of the reagents to the catalytically active sites as a function of their solubility in the ionic layer. Therefore, the primary products (butenes) formed during the hydrogenation of 1,3-butadiene are extracted from the ionic layer by the 1,3-butadiene (which is at least four times more soluble in the ionic phase than the butenes). This catalytic system [Pd(0) nanoparticles embedded in ionic liquids] is one of the most effective for performing the selective hydrogenation of 1,3-butadiene to 1-butene. Most important, we have demonstrated that the hydrogenation of butadiene can be used as a chemical probe to check the character-

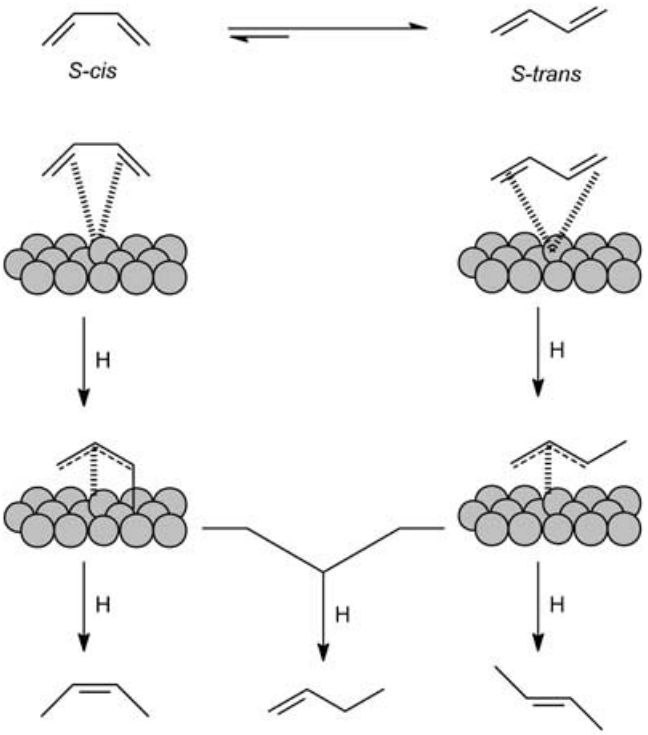

Scheme 2. Proposed reaction pathways involved in the partial hydrogenation of butadiene in the catalyst surface through 1,2- and 1,4-additions on *S-cis* and *S-trans* conformers of butadiene leading to different π-allyl intermediates.

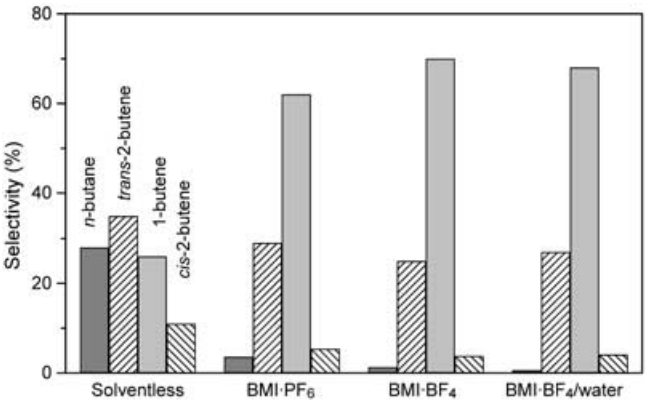

Figure 11. Reaction products selectivity obtained from the hydrogenation of 1,3-butadiene (at 85% conversion) by Pd(0) nanoparticles (5 mg) in different reaction media at 40 °C and 4 atm.

istic behaviour of soluble Pd(0) nanoparticles, i.e., if they possess a more pronounced surface-like or single site-like properties. Although simple 1,3-dialkylimidazolium ionic liquids do not provide an effective protection to the nanoparticles against aggregation under the catalytic reaction conditions, it can be anticipated that the use of functionalized imidazolium ionic liquids may provide an effective nanoparticle protection

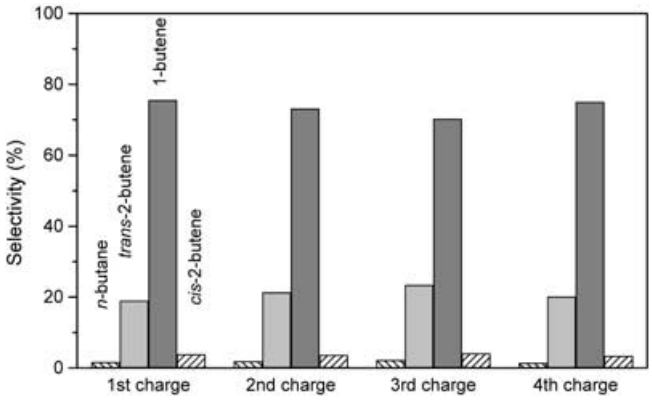

Figure 12. Selectivity at 85% conversion in 1,3-butadiene hydrogenation under biphasic reaction conditions (1×10^{-3} mL of $BMI \cdot BF_4$, 40 °C, 4 atm H_2).

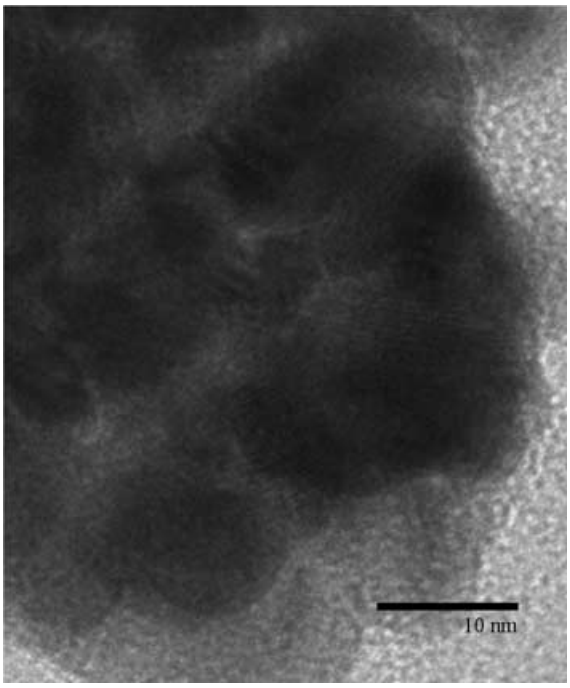

Figure 13. TEM micrograph of Pd(0) nanoparticles dispersed in $BMI \cdot PF_6$ recovered after three charges of 1,3-butadiene.

against aggregation as recently demonstrated in the case of C–C coupling reactions promoted by nanoscale palladium catalysts dissolved in functionalized pyridinium ionic liquids.[13]

Experimental Section

Materials

All bench procedures were carried out under Ar using Schlenk techniques. The ionic liquids $BMI \cdot BF_4$ and $BMI \cdot PF_6$ were prepared according to the procedure described in the literature[14]

and their purity checked by the $AgNO_3$ test and cyclic voltametry. All other chemicals were acquired from commercial sources. The 1,3-butadiene used was distilled before the hydrogenation reactions. The GC analyses were performed in a Shimadzu GC 14-B with a 30 m alumina Megabor column using H_2 as mobile phase. The hydrogenation reactions products were separated under 4 psig and 40 °C isotherm. Products were identified by patterns. The powder XRD analyses were performed in a Philips X'Pert MRD using the Bragg-Brentano geometry and a graphite crystal as monochromator. The chemical analysis of the nanoparticles was obtained by XPS using the VG ESCALAB MkII, equipped with 150 mm hemispherical analyser and Al K_α anode X-ray source. The overall resolution was 200 meV. The TEM analyses were performed in a JEOL JEM 2010 transmission electron microscope operating at 200 kV with nominal resolution of 0.25 nm. Samples for TEM were prepared by deposition of the Pd(0) nanoparticles dispersed on dichloromethane and a drop of this solution was transferred on a holey carbon grid.

Synthesis of the Pd(0) Nanoparticles

The Pd(0) nanoparticles were synthesized by the reduction of $Pd(acac)_2$ dissolved in $BMI \cdot PF_6$ by molecular hydrogen. In a typical experiment, 2 mL of $BMI \cdot PF_6$ were added to a solution of 30 mg (0.1 mmol) in methanol (ca. 1 mL) in a modified Fischer–Porter bottle reactor. The formed solution was held at 100 °C for 10 minutes and volatiles were removed under reduced pressure. The system was cooled, held at 75 °C, and H_2 (4 atm) was admitted to the reactor bottle for 5 minutes. The reduction of $Pd(acac)_2$ was followed by the formation of a black powder suspension in the ionic liquid. The formed black powder was filtered by centrifugation (3000 rpm, 15 min, 3 times) and washed with dichloromethane 2×10 mL and 5×10 mL and dried under reduced pressure. The total yield was 10 mg ($>98\%$ of the initial Pd content). The nanoparticles were analysed by powder X-ray diffraction and transmission electron microscopy.

Hydrogenation Reactions

Hydrogenations experiments were performed in a modified Fischer–Porter bottle connected to a constant pressure feed reservoir.

Solvent-Free Conditions: In a typical experiment, 5 mg of the Pd(0) nanoparticles and 2.7 g (50 mmol) of 1,3-butadiene were added to the reactor bottle and H_2 (4 atm) was admitted to the system. The temperature in the active phase was held at 40 ± 1 °C and the temperature in the neck of the bottle was held at 25 ± 1 °C. Samples of the gas phase were collected by a manually operated valve on the head of the reactor and analysed by GC.

Nanoparticles Dispersed or Embedded in the Ionic Liquids: The reactions performed with the nanoparticles dispersed in the ionic liquids were performed using the same experimental set-up. In these cases the isolated nanoparticles were directly dispersed in the desired amount (using a syringe or micro-syringe) placed in the Fischer–Porter bottle.

Acknowledgements

Thanks are due to CNPq, CT-PETRO and FAPERGS for partial financial support and to CAPES for a scholarship do A. P. U.

References and Notes

[1] See for example: a) G. G. Cervantes, F. J. C. S. Aires, J. C. Bertolini, *J. Catal*. **2003**, *214*, 26–32; b) D. C. Lee, J. H. Kim, W. J. Kim, J. H. Kang, S. H. Moon, *Appl. Catal. A: Gen.* **2003**, *244*, 83–91; c) M. Schmal, D. A. G. Aranda, R. R. Soares, F. B. Noronha, A. Frydman *Catal. Today* **2000**, *57*, 169–176; d) J. F. Ciebien, R. E. Cohen, A. Duran, *Mater. Sc. Eng. C* **1999**, *7*, 45–50; e) ; A. Sarkany, Z. Zsoldos, G. Stefler, J. W. Hightower, L. Guzci *J. Catal.* **1995**, *157*, 179–189; f) B. K. Furlong, J. W. Hightower, T. Y.-L. Chan, A. Sarkany, L. Guczi, *Appl. Catal. A: Gen.* **1994**, *117*, 41–51; g) M. M. Pereira, F. B. Noronha, M. Schmal *Catal. Today* **1993**, *16*, 407–415; h) A. Borgna, B. Moraweck, J. Massadier, A. J. Renouprez, *J. Catal.* **1991**, *128*, 99–112.

[2] a) J. J. Phillips, P. B. Wells, G. R. Wilson, *J. Chem. Soc. A* **1969**, 1351; b) B. J. Joice, J. J. Rooney, P. B. Wells, G. R. Wilson, *Disc. Faraday Soc.* **1966**, 223.

[3] For a review, see: A. Molnar, A. Sarkany, M. Varga, *J. Mol. Catal. A: Chem.* **2001**, *173*, 185–221.

[4] For regioselective reductions by transition-metal complexes in ionic liquids see, for example: a) Y. Chauvin, L. Mussmann, H. Olivier, *Angew. Chem. Int. Ed. Engl.* **1995**, *34*, 2698–2700; b) S. Steines, P. Wasserscheid, B. Driessen-Holscher, *J. Prak. Chem.* **2000**, *342*, 348–354; c) H. Berthold, T. Schotten, H. Hönig, *Synthesis* **2002**, 1607–1610; d) K. Anderson, P. Goodrich, C. Hardacre, D. W. Rooney, *Green.Chem.* **2003**, *5*, 448–453; e) C. S. Consorti, A. P. Umpierre, R. F. de Souza, J. Dupont, P. A. Z. Suarez, *J.Braz.Chem.Soc.* **2003**, *14*, 401–405; f) D. B. Zhao, Z. F. Fei, R. Scopelliti, P. J. Dyson, *Inorg. Chem.* **2004**, *43*, 2197–2205; g) D. B. Zhao, Z. F. Fei, C. A. Ohlin, G. Laurenczy, P. J. Dyson, *Chem. Commun.* **2004**, 2500–2501; h) D. Zhao, P. J. Dyson, G. Laurenczy, J. S. McIndoe, *J. Mol. Catal. A: Chem.* **2004**, *214*, 19–25.

[5] G. W. Parshall, *J. Am. Chem. Soc.* **1972**, *94*, 8716–8719.

[6] a) J. Dupont, R. F. de Souza, P. A. Z. Suarez, *Chem. Rev.* **2002**, *102*, 3667–3691; b) J. Dupont, J. Spencer *Angew. Chem. Int. Ed.* **2004**, *43*, 5296–5297; c) J. Dupont, *J. Braz. Chem. Soc.* **2004**, *15*, 341–350.

[7] J. Dupont, P. A. Z. Suarez, A. P. Umpierre, R. F. de Souza, *J. Braz .Chem. Soc.* **2000**, *11*, 293–297.

[8] A. T. Bell, *Science*, **2003**, *299*, 1688–1691.

[9] For soluble Pd nanoparticles, see: S. Jansat, M. Gomez, K. Philippot, G. Muller, E. Guiu, C. Claver, S. Castillon, B. Chaudret, *J. Am. Chem. Soc.* **2004**, *126* 1592–1593.

[10] For review about soluble transition-metal nanoparticles, see: A. Roucoux, J. Schulz, H. Patin, *Chem. Rev.* **2002**, *102* 3757–3778.

[11] J. Huang, T. Jiang, B. X. Han, H. X. Gao, Y. H. Chang, G. Y. Zhao, W. Z. Wu, *Chem. Commun.* **2003**, 1654–1655.

[12] a) J. Dupont, G. S. Fonseca, A. P. Umpierre, P. F. P. Fichtner, S. R. Teixeira, *J. Am. Chem. Soc.* **2002**, *124*, 4228–4229; b) G. S. Fonseca, A. P. Umpierre, P. F. P. Fichtner, S. R. Teixeira, J. Dupont, *Chem. Eur. J.* **2003**, *9*, 3263–3269; c) C. W. Scheeren, G. Machado, J. Dupont, P. F. P. Fichtner, S. R. Texeira, *Inorg. Chem.* **2003**, *42*, 4738–4742; d) L. M. Rossi, G. Machado, P. F. P. Fichtner, S. R. Teixeira, J. Dupont, *Catal. Lett.* **2004**, *92*, 149–155; e) E. T. Silveira, A. P. Umpierre, L. M. Rossi, G. Machado, J. Morais, G. V. Soares, I. J. R. Baumvol, S. R. Teixeira, P. F. P. Fichtner, J. Dupont, *Chem. Eur. J.* **2004**, *10*, 3734–3740.

[13] D. B. Zhao, Z. F. Fei, T. J. Geldbach, R. Scopelliti, P. J. Dyson, *J. Am. Chem. Soc.* **2004**, *126*, 15876–15882.

[14] P. A. Z. Suarez, J. E. L. Dullius, S. Einloft, R. F de Souza, J. Dupont, *Polyhedron* **1996**, *15*, 1217–1219; b) J. Dupont, P. A. Z. Suarez, C. S. Consorti, R. F. de Souza, *Org. Synth.* **2002**, *79*, 236–243.

